Tribological behavior of polymers simulated by molecular dynamics

Witold Brostow,[a] J. Adam Hinze, and Ricardo Simões
Laboratory of Advanced Polymers and Optimized Materials (LAPOM), Department of Materials Science & Engineering, University of North Texas, Denton, Texas 76203-5310

(Received 9 July 2003; accepted 25 November 2003)

Using molecular dynamics to simulate behavior of polymer surfaces during scratch testing, we report the first results of computer simulations of scratch behavior of noncrystals. A previously described procedure for creating realistic polymeric materials on the computer [W. Brostow, A.M. Cunha, and R. Simoes, Mater. Res. Innovat. **7,** 19 (2003)] and used until now to simulate mechanical behavior of metals [S. Blonski, W. Brostow, and J. Kubat, Phys. Rev. B **49,** 6494 (1994)] and one- and two-phase polymers [W. Brostow, A.M. Cunha, J. Quintanilla, and R. Simoes, Macromol. Theory Simul. **11,** 308 (2002); W. Brostow, A.M. Cunha, and R. Simoes, Proc. Ann. Tech. Conf. Soc. Plastics Engrs. **60,** 3105 (2002)] was applied. While experiments provide only the macroscopic penetration depth and the recovery (healing) depth, the simulations give the behavior of each macromolecular chain segment at each moment in time. We report results for one-phase polymers and also for systems with varying concentrations of a liquid crystalline (LC) second-phase that acts as a reinforcement. We relate the local structure to scratch resistance and recovery. The orientation of the chemical bonds is a major factor. The presence of a LC phase improves the tribological properties; however, the effect is not as significant as might have been expected.

I. INTRODUCTION

The tribological properties of materials are important for their service performance—as argued eloquently and in detail by Rabinowicz.[1] However, his book deals almost exclusively with metals, and metal surfaces are not easily scratched anyway. A Swiss collective book on tribology[2] has only one short chapter on polymers, mostly data tabulation of friction values. A book by Goldman on polymeric materials covers a large variety of deformation modes but says little about tribological properties.[3] While Teflon is widely used because of its low friction, its scratch resistance is quite poor.[4] Scratch resistance is particularly important; a scratch may acquire the role of a crack and become the origin of crack propagation.[5,6]

The polymer tribology we need to develop has to be based on chemical structures of the polymeric materials. Otherwise, all practical applications would be condemned to a trial-and-error procedure: mixing something with something else and "hoping for the best." Such an approach represents a significant time and resource investment—and for many cases will not result in any improvement over the initial properties of a material.

One obtains two values from performing an experiment: the instantaneous penetration depth R_p and the residual (healing) depth R_h.[4,7,8] However, testing does not provide any information about the evolution of that recovery from the instant the indenter hits the material through the moment when total recovery has occurred. Moreover, experiments do not provide connections between macroscopic tribological properties and the material structure at the molecular level.

We have previously reported results of computer simulations of mechanical behavior of polymers including polymer liquid crystals (PLCs).[9,10,11] These simulations have shown us how mechanical properties of the material depend on its structure. As argued by Fossey,[12] one of the main advantages of computer simulations is the possibility of obtaining information that is not readily available experimentally. Termonia has used computer simulations to study the unusual combination of high mechanical strength, stiffness, and elongation at break of the spider silk dragline structure.[13] We describe in this paper a method for simulating scratching behavior in polymeric materials—thus the first computer simulations of behavior of noncrystalline materials during a scratching test. By combining simulation results inaccessible

[a] Address all correspondence to this author.
e-mail: brostow@ unt.edu

experimentally with those from experiments, we expect to achieve understanding of the scratching behavior necessary for development of polymers with improved scratch resistance.

Our survey of literature on computer simulations of tribological properties has led us to a number of papers that, with one exception, deal with friction. Tupper and Brenner[14] have investigated friction for self-assembled monolayer films. They have concluded that the structure of the film changes during compression; however, that does not significantly affect the friction properties. Simulations of friction in monolayer films have also been reported by Koike and Yoneya.[15] They have concluded that the van der Waals interactions are the main cause of differences between the frictional forces for different monolayers. Gerde and Marder[16] used molecular dynamics (MD) simulations to investigate friction and its connection to the mechanism of self-healing cracks. Their simulations are based on a self-healing crack moving along the interface between the two surfaces, leading to slip between the solids. They have thus obtained dynamic friction (steady-state) values from an atomic scale simulation.

There is one report of nanoscale scratching simulation. Komanduri et al.[17] investigated single-crystal aluminum in this way. Their results show how different crystal orientations and scratch directions yield different values of tribological properties. Because polymers are never fully crystalline, their results are of limited use in polymer tribology.

II. SIMULATION MODEL

Our simulations are based on the MD method originally developed by Alder and Wainwright.[18] The reasons for our preference over the Monte Carlo method have been explained in detail in previous papers.[10,19] In the MD method all particles are moved simultaneously, and each particle is defined by three Cartesian coordinates of position and three coordinates of momentum. It is thus possible to track the displacement of each particle along time. The MD method uses pairwise interactions between the particles in the system which determine the total force applied on each particle due to interactions with its neighbors. For reasons explained before,[9] we use the three-dimensional triangular lattice; thus, each particle in the system has 12 nearest neighbors (not accounting for point defects).

Four different interaction potentials have been defined for our polymeric materials. We consider intrachain (chemical) and interchain (van der Waals) interactions as well as different behavior for rigid and flexible bonds in two-phase materials. To characterize the intrachain rigid bonds we have incorporated a Morse-like potential with a relatively narrow well. For the intrachain flexible bonds we introduced a spliced double-well potential, allowing for *cis* to *trans* conformation changes over a potential barrier. The weak van der Waals bonds between chains are defined by a Morse-like potential, in this case with a relatively broad well. The bond strengths for these secondary interactions are different for rigid and flexible segments. We treat the interaction between a rigid and a flexible segment as rigid.

The molecular dynamics simulation code used for these simulations was developed by us, based on the models by Cook et al.[20,21] modified by Blonski and one of us for the simulation of PLCs.[22] A detailed description of our simulation model, including the interaction potentials used and the equations of motion, has been provided elsewhere.[19] We use reduced units as defined in a previous paper.[9] We maintain the temperature via kinetic energy and a coupling to a temperature bath as previously described elsewhere.[9]

III. MATERIAL GENERATION

The material generation procedure we use is based on an approach developed by Mom.[23] We apply this approach for the construction of self-avoiding polymer chains on the three-dimensional triangular lattice. Following the approach advocated by Flory,[24] we use a united atom model so that each segment in the material corresponds to a statistical segment that represents a small part of a polymeric chain. In the beginning of the generation procedure, each of the lattice sites represents one chain consisting of a single segment. The system is searched for the two nearest end segments of all chains. Those two segments are then connected, forming a two-segment chain and decreasing the number of chains in the system by one. The search procedure is repeated until no more chains of length two can be created. Then the maximum length of chains is increased by one and the search for the two nearest end segments of chains restarts. These steps are repeated until there are no more neighboring segments in two different chains that can be connected.

The procedure results in a three-dimensional material of self-avoiding randomly oriented chains, each chain containing a certain number of segments (Fig. 1). The material thus created usually presents also vacancies corresponding to segments in lattice sites that were never connected to chains due to the random nature of the generation process. The presence of these vacancies is an important feature to represent adequately real materials. For details of the material generation procedure and realistic features of the resulting materials see Ref. 25.

After creation of the polymer chains structure, a rigid liquid-crystalline (LC) second phase can be added to the flexible matrix. The LC-rich phase was found experimentally[26] to form quasi-spherical agglomerates, which are usually called islands. In our computer-generated

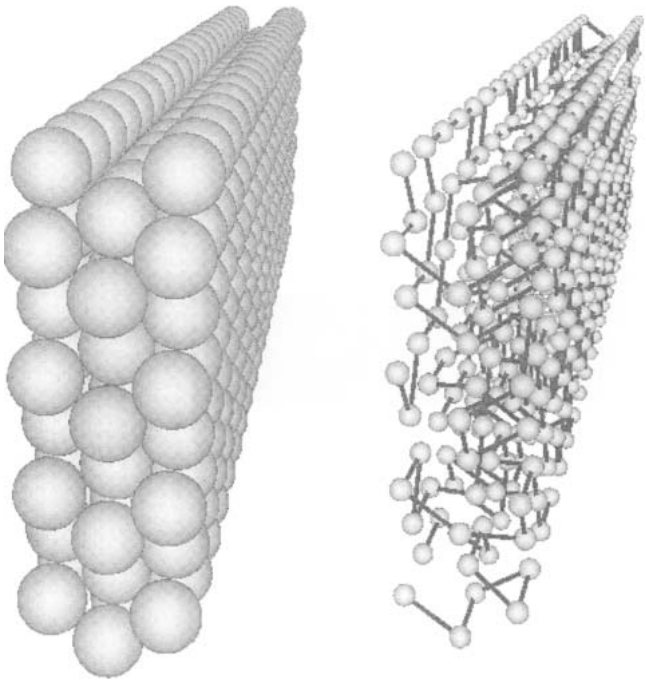

FIG. 1. A snapshot of the computer-generated polymeric material (on the left) and its coiled chain structure (on the right).

materials, the LC islands are created as polyhedra, and incorporated by random sequential addition. The details of the second phase addition procedure have thoroughly been explained elsewhere.[25]

Due to the random nature of the island placement algorithm, the material sometimes exhibits some regions of high LC concentration and other regions with low LC concentration. The second phase distribution has been shown before to influence significantly the mechanical properties of the material.[10] Thus, one can expect that it will also affect the tribological properties.

IV. SCRATCHING SIMULATION PROCEDURE

To simulate the scratching behavior, a perpendicular external force is applied on a surface of the material and moved along that surface. One could equally create a virtual indenter on the computer and move it against the surface. However, by representing the indenter as a force applied directly on the surface segments, we eliminate effects of the size and shape of the scratching tool.

The total force on a given particle is the sum of the forces resulting from pairwise interactions and any external forces applied:

$$F_{ij}(t) = \frac{-\mathrm{d}U_c(t)}{\mathrm{d}R_{ij}} + F_{ij}^{ext} \quad . \tag{1}$$

Here, F_{ij} is the force acting on the ith segment of the jth chain at time t, U_c is the total configurational energy of the system (the sum of pairwise interactions), R_{ij} is the current location of the segment in question, and F_{ij}^{ext} is the external force imposed. For the simulations reported in this paper, the external scratching force was kept constant at the value of 10. Goldman[27] defines the linear viscoelastic behavior by the dependence of the stress/strain ratio on time only. We shall show in future papers with varying force that this condition is not fulfilled in the range of forces we apply; we are outside the linear viscoelastic region.

As we do in experiments, we avoid edge effects along the scratching axis by not starting the scratching procedure at an edge. We begin at the fifth segment along the scratching axis and we stop at the fifth segment before the end of the surface. Because scratching is done along the x axis and the force is applied on the y axis, we move the force along the center layer of the material along the z axis, to avoid edge effects along this axis. This center layer is defined as the scratching layer. We define scratching path as the series of segments of the scratching layer on which force will be applied, one at a time.

The material is initially created with all segments positioned in ideal triangular lattice positions. Because this is not realistic, a random perturbation is introduced by slightly shifting the position of all segments by a small random value (less than 1% of the equilibrium distance between segments). The first simulation step is then run without any external forces applied to allow the system to reach equilibrium. Then, the scratching force is applied to the first segment on the scratching path. At each simulation step, the scratching force is displaced to the next segment on the scratching path. After the scratching force has been applied to the last such segment, it is removed and the material is allowed to recover. This recovery stage without any external forces applied lasts for 10 simulation steps, which was found sufficient to allow the segments on the scratching path to fully recover. We have defined a segment as having fully recovered when the position of that segment changes less than 1% between two consecutive simulation steps.

Our simulation program allows the force to be kept for any specified amount of time in each segment on the scratching path to simulate different scratching rates. Similarly, the value of the scratching force can be specified by the user. In future publications we shall report on the effect of these two parameters on the tribological properties.

In Fig. 2, we observe the recovery of the material from time t_0—corresponding to the force removal after scratching—to time t_9, nine time-steps later. Higher depths at the right side of the material are due to a shorter time span since the passage of the indenter; the indenter is moving from left to right.

We can look at the viscoelastic recovery for individual segments. Each segment displays a different penetration depth according to the local chain geometry and the

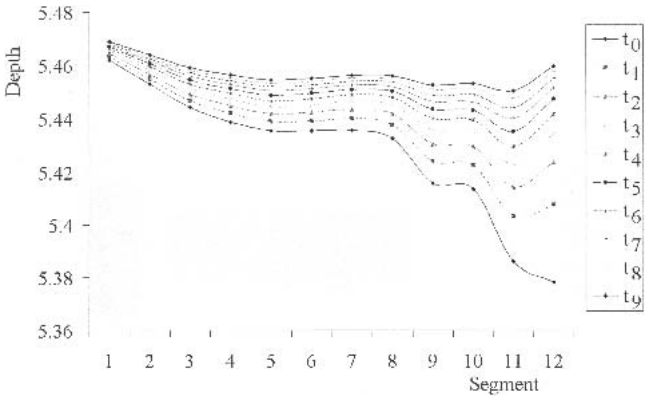

FIG. 2. Viscoelastic recovery of the material after scratching. The t_9 line corresponds to the final topography of the surface after full recovery.

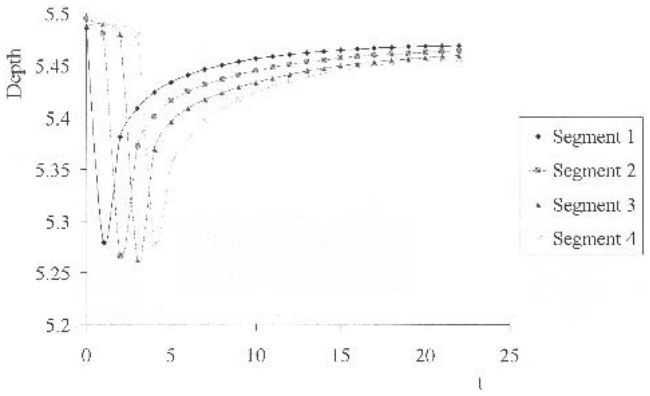

FIG. 3. Displacement along time of some segments on the scratching path of a simulated material. Note the different penetration depth values for each segment. Note also the clear viscoelastic nature of the recovery process.

presence of neighboring LC-rich islands. In Fig. 3 we represent the displacement of some segments on the scratching path of a simulated material. For ease of visualization, only the first few steps of the simulation are shown. It is clear at what moment the force was applied to each segment—that segment is displaced deeply into the material. We observe significant recovery immediately when the force representing the indenter moves to another segment and further slower recovery up to a plateau. Clearly, the deepest location of a segment at the "bottom of a well" corresponds to the experimental penetration depth R_p whereas the plateau level corresponds to the residual or healing depth R_h.

V. SELECTED RESULTS

Due to the random nature of the material generation process, the local chain geometry of the segments on the scratching path varies from segment to segment. Naturally, it also varies from material to material. The scratch resistance and recovery are related to the local molecular structure, in particular to the intrachain bonds (primary interactions) of the segments on the scratching path.

Even in a fully flexible material, each segment on the scratching path exhibits a different behavior under the same force level. The difference can in fact be substantial from one segment to the next, as can be seen in Fig. 4. In this figure, R_0 corresponds to the topography of the surface; that is, the position of the segments on the scratching path before scratching began. The difference between the penetration depth and the residual depth is the permanent deformation resulting from the scratch. Experiments[7] provide us with these three values: R_0, R_p, and R_h.

The situation calls for more extensive future studies. Goldman[28] has presented convincing experimental evidence about the role of entanglements in polymer mechanical behavior. The same may apply to tribological behavior—and only simulations provide the capability to make clear connections between macroscopic and molecular levels.

The different behavior in the penetration depth along the scratching path can only mean that the spatial structure of the chains influences the behavior of the segments. The local intrachain bond geometry of the chains is represented in Fig. 5. For perspicuity, only bonds to segments in the scratching path are included.

We find at least two relevant kinds of behavior of segments: when a segment on the scratching path is bonded to a segment immediately below it on the scratching layer (segments 6, 7, 8, 10, and 12 in Fig. 5) or else when the segment on the scratching path is bonded in some other way.

Our analysis of the simulation results reveals that in the first case (segments 6, 7, 8, 10, and 12), the segments exhibit significantly reduced penetration depth; see again Fig. 4. This appears to be the most advantageous chain geometry for improved scratch properties. For all other bond geometries, the segments behave similarly and display relatively higher penetration depths.

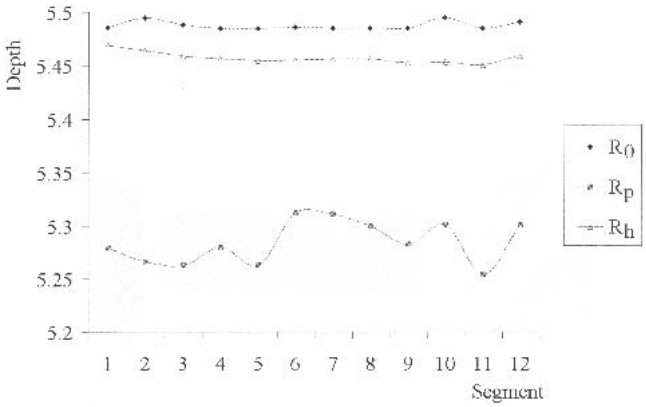

FIG. 4. Initial surface topography, penetration depth, and recovery depth for the segments along the scratching path for the purely flexible material.

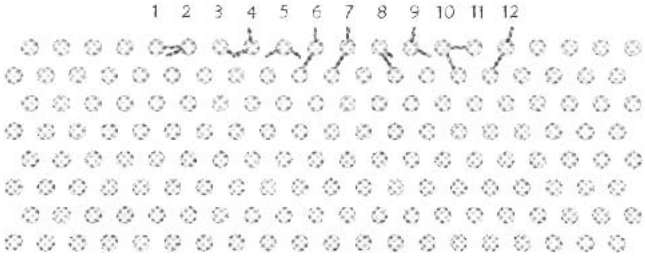

FIG. 5. Local chain structure for each of the 12 segments on the scratching path of the fully flexible material.

The presence and distribution of the rigid phase on the flexible matrix also influences the properties and behavior of the material.[29,30] To study the presence and distribution of a rigid second phase, we compared the results obtained for single-phase materials with those containing different LC concentrations. We have used the same chain structure for all these materials to isolate the effect of the concentration. This is in fact one of the greatest advantages of computers simulations—we can change different variables one at a time independently of other variables.

Let us now compare the fully flexible material previously studied and a material with the same chain structure but containing 25% LC segments. The structure of the scratching layer of this material is shown in Fig. 6. We can observe the distribution of the LC islands beneath the twelve segments on the scratching path. It is clear that the islands are not homogeneously distributed throughout the material; some segments on the scratching path have mostly flexible segments beneath them whereas others have a large number of islands directly beneath them.

We have found that segments in flexible regions of the material exhibit similar behavior for the single-phase flexible material or one containing LC islands. Only when islands exist below a segment on the scratching path will that segment exhibit a different behavior compared to the fully flexible material. In that case, when the external force is applied to the segment on the scratching path located above an island, we observe a shallower scratch—a reduction in both the penetration depth and the recovery depth. Thus, the rigid LC islands are performing their role as a reinforcement, as could be expected. This effect is shown in Fig. 7. We compare here the results for the fully flexible material and one containing LC islands. We see that the two groups of segments on the scratching path—segments 4, 5, and 6, and also segments 10, 11, and 12—that have rigid islands below them exhibit a lower penetration depth. Other segments display behavior similar to their counterparts in the fully flexible material.

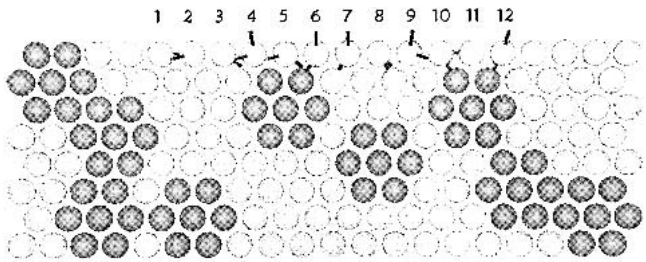

FIG. 6. Rigid LC island distribution on the scratching layer and local chain structure for each of the 12 segments on the scratching path of the 25% LC material.

The presence of the LC islands indeed improves scratch resistance and recovery, even if not very significantly. However, it is not the concentration of the LC phase but the island spatial distribution that determines the tribological properties of the material. We find that if the islands are deep into the material—more than one flexible segment between them and the surface segments on the scratching path—the reinforcement is negligible. It seems that preferential migration of the second phase to the surface of the material would be desired for improved scratch resistance.

VI. CONCLUSIONS

As contrasted with the scratching experiments that provide only two averages per material, that is, the averages of R_p and R_h, in the simulations we follow the behavior of each segment scratched by the indenter as a continuous function of time. There is a direct connection to experiments because R_p and R_h for each segment are visible, too, and can be averaged over the material surface. This is clearly only a beginning; much more can be learned from scratching simulations for materials with various predefined morphologies.

At least one more aspect deserves to be mentioned at this time. Wetting angle experiments for three liquids (two polar) for a given surface can be used to calculate the surface tension γ of the respective polymer solid.[31] Our such calculations for an epoxy with additives show

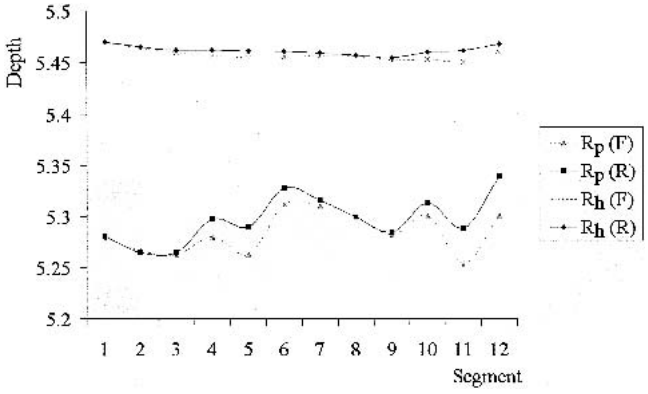

FIG. 7. Penetration and recovery depth for the segments along the scratching path for the purely flexible and the 25% LC materials.

connections between γ on one hand and R_p, R_h, static friction, and dynamic friction on the other.[32] Because γ is determined by the interactions at and near the surface, this is one more dimension of polymer tribology which can be elucidated by simulations.

ACKNOWLEDGMENTS

Support for this research has been provided by the Fundação para a Ciência e a Tecnologia, 3° Quadro Comunitário de Apoio, Lisbon, and also by the Robert A. Welch Foundation, Houston (Grant No. B-1203).

REFERENCES

1. E. Rabinowicz, *Friction and Wear of Materials*, 2nd ed. (Wiley, New York, 1995).
2. *Matériaux et contacts: une approche tribologique*, edited by G. Zambelli and L. Vincent (Presses polytechniques universitaires romandes, Lausanne, 1998).
3. A.Y. Goldman, *Prediction of Deformation Properties of Polymeric and Composite Materials* (American Chemical Society, Washington, DC, 1994).
4. W. Brostow, G. Damarla, J.A. Howe, and D. Pietkiewicz (unpublished).
5. *Failure of Plastics*, edited by W. Brostow and R.D. Corneliussen (Hanser, Munich—Vienna—New York, 1986).
6. *Performance of Plastics*, edited by W. Brostow (Hanser, Munich—Cincinnati, 2000).
7. W. Brostow, B. Bujard, P.E. Cassidy, H.E. Hagg, and P.E. Montemartini, Mater. Res. Innovat. **6,** 7 (2002).
8. W. Brostow, B. Bujard, P.E. Cassidy, and S. Venumbaka, Int. J. Polym. Mater. (2003, in press).
9. S. Blonski, W. Brostow, and J. Kubat, Phys. Rev. B **49,** 6494 (1994).
10. W. Brostow, A.M. Cunha, J. Quintanilla, and R. Simoes, Macromol. Theory Simul. **11,** 308 (2002).
11. W. Brostow, A.M. Cunha, and R. Simoes, Proc. Ann. Tech. Conf. Soc. Plastics Engrs. **60,** 3105 (2002).
12. S. Fossey, in *Performance of Plastics*, edited by W.Brostow (Hanser, Munich—Cincinnati, 2000), p. 63.
13. Y. Termonia, Macromolecules **27,** 7378 (1994).
14. K.J. Tupper and D.W. Brenner, Thin Solid Films **253,** 185 (1994).
15. A. Koike and M. Yoneya, J. Chem. Phys. **105,** 6060 (1996).
16. E. Gerde and M. Marder, Nature **413,** 285 (2001).
17. R. Komanduri, N. Chandrasekaran, and L.M. Raff, Wear **240,** 113 (2000).
18. B.J. Alder and T.E. Wainwright, J. Chem. Phys. **27,** 1208 (1957).
19. W. Brostow, M. Donahue III, C.E. Karashin, and R. Simoes, Mater. Res. Innovat. **4,** 75 (2001).
20. R. Cook and M.B. Mercer, Mater. Chem. Phys. **12,** 571 (1985).
21. R. Cook, J. Polymer Sci. **26,** 1988 (1988).
22. S. Blonski and W. Brostow, J. Chem. Phys. **95,** 2890 (1991).
23. V. Mom, J. Comput. Chem. **2,** 446 (1981).
24. P.J. Flory, *Statistical Mechanics of Chain Molecules* (Wiley-Interscience, New York, 1969).
25. W. Brostow, A.M. Cunha, and R. Simoes, Mater. Res. Innovat. **7,** 19 (2003).
26. W. Brostow, T.S. Dziemianowicz, J. Romanski, and W. Werber, Polymer Eng. Sci. **28,** 785 (1998).
27. A.Y. Goldman, in *Performance of Plastics*, edited by W. Brostow (Hanser, Munich—Cincinnati, 2000), Chapter 7.
28. A.Y. Goldman and K. Venkatashan, Proc Ann Tech Conf Soc Plastics Engrs. **60,** 1363 (2002).
29. W. Brostow, T.S. Dziemianowicz, R. Romanski, and W. Werber, Polymer Eng. Sci. **28,** 785 (1988).
30. M. Hess, in *Performance of Plastics*, edited by W. Brostow (Hanser, Munich—Cincinnati, 2000), p. 519.
31. R.J. Good, in *Contact Angle, Wettability and Adhesion*, edited by K.L. Mittal (VSP, New York, 1993), Chapter 1.
32. W. Brostow, P.E. Cassidy, J. Macossay, D. Pietkiewicz, and S. Venumbaka, Polymer Int. **52,** 1498 (2003).